Published OnlineFirst November 13, 2012; DOI: 10.1158/0008-5472.CAN-12-2184

Cancer Research

RNA Trafficking by Acute Myelogenous Leukemia Exosomes

Jianya Huan[1,4], Noah I. Hornick[1,4], Matthew J. Shurtleff[1], Amy M. Skinner[1,4], Natalya A. Goloviznina[1,4], Charles T. Roberts Jr[1,2,3,5], and Peter Kurre[1,2,4]

Abstract

Extrinsic signaling cues in the microenvironment of acute myelogenous leukemia (AML) contribute to disease progression and therapy resistance. Yet, it remains unknown how the bone marrow niche in which AML arises is subverted to support leukemic persistence at the expense of homeostatic function. Exosomes are cell membrane–derived vesicles carrying protein and RNA cargoes that have emerged as mediators of cell–cell communication. In this study, we examined the role of exosomes in developing the AML niche of the bone marrow microenvironment, investigating their biogenesis with a focus on RNA trafficking. We found that both primary AML and AML cell lines released exosome-sized vesicles that entered bystander cells. These exosomes were enriched for several coding and noncoding RNAs relevant to AML pathogenesis. Furthermore, their uptake by bone marrow stromal cells altered their secretion of growth factors. Proof-of-concept studies provided additional evidence for the canonical functions of the transferred RNA. Taken together, our findings revealed that AML exosome trafficking alters the proliferative, angiogenic, and migratory responses of cocultured stromal and hematopoietic progenitor cell lines, helping explain how the microenvironmental niche becomes reprogrammed during invasion of the bone marrow by AML. *Cancer Res; 73(2); 1–12. ©2012 AACR.*

Introduction

Although the majority of patients with acute myelogenous leukemia (AML) achieve remission, nearly half will die from disease relapse. The contribution of microenvironmental cues to the survival, spread, and relapse of AML in the marrow are increasingly recognized as crucial in the process of leukemic evolution (1, 2). The bone marrow is structurally and functionally specialized to sustain lifelong hematopoietic and immune function; its infiltration by leukemia is associated with the acquisition of unique properties that make the bone marrow a sanctuary for persistent disease (3, 4). Even as differences emerge that distinguish the leukemic microenvironment from the homeostatic hematopoietic stem cell (HSC) niche, the mechanisms whereby malignant cells reprogram the niche remain to be clarified (4–6). Instances of extrinsic resistance are illustrated in the treatment of high-risk AML associated with internal tandem duplication (ITD) mutations in FMS-like tyrosine kinase 3 (FLT3), in which specific inhibitors eliminate circulating blasts without eradicating leukemic cells in the bone marrow (7). Conversely, FLT3-ITD^{pos} AML cells are sensitized to the tyrosine kinase inhibitor sorafenib by inhibition of chemokine receptor-4 (CXCR4)-SDF-1α niche signaling with bone marrow stromal cells (2). Although integrin-, chemokine-, and cytokine-mediated adhesive and paracrine interactions all contribute to drug resistance, none of these fully address how marrow invasion by leukemia cells results in niche remodeling (6).

Conventional intercellular signaling relies on direct cell–cell contact or the action of secreted molecules, but more recent studies indicate an additional, evolutionarily conserved mechanism whereby cells communicate via the exchange of extracellular vesicles carrying protein and RNA cargo (8, 9). As a unique consequence of cell–cell vesicle trafficking, the cytoplasmic delivery of mRNA, miRNA, or protein can circumvent transcriptional controls. Vesicle trafficking of receptors between cells, for example, may transcend niche signaling that is based on conventional restrictions of cell-specific ligand or receptor expression and modulate growth factor signaling cascades. Vesicles ranging in size from 30 to 100 nm (exosomes) to 100 to 1,000 nm (broadly termed microvesicles) have been detected in the urine and plasma of patients with diverse malignancies (10). However, detailed studies of vesicle biology in AML have not been reported (11, 12).

The results presented here show the release of exosome-sized vesicles by AML cells and illustrate how vesicle trafficking alters gene expression, protein secretion, and behavior of

Authors' Affiliations: Departments of [1]Pediatrics, [2]Cell & Developmental Biology, and [3]Medicine; [4]Papé Family Pediatric Research Institute, Oregon Health & Science University, Portland; and [5]Oregon National Primate Research Center, Beaverton, Oregon

Note: Supplementary data for this article are available at Cancer Research Online (http://cancerres.aacrjournals.org/).

Prior presentation: This work was presented, in part, at the 2011 meeting of the American Society of Hematology.

Corresponding Author: Peter Kurre, Department of Pediatrics and Papé Family Pediatric Research Institute, Oregon Health & Science University, 3181 SW Sam Jackson Park Rd., Portland, OR 97239. Phone: 503-494-7655; Fax: 503-494-0714; E-mail: kurrepe@ohsu.edu

doi: 10.1158/0008-5472.CAN-12-2184

Published OnlineFirst November 13, 2012; DOI: 10.1158/0008-5472.CAN-12-2184

bystander cells. We show that vesicles contain diverse RNA species, including mRNAs and miRNAs relevant to AML biology and with broad biomarker potential. In aggregate, our work indicates that trafficking of AML exosomes elicits broad functional changes in bystander cells.

Materials and Methods

Cell lines and cell culture

AML cell lines (HEL, HL-60, Molm-14, and U937) were provided by Dr. Jeffrey (Oregon Health & Science University) Tyner and cultured in RPMI (Invitrogen) with 10% vesicle-free FBS. Vesicle-free FBS was produced by centrifugation of FBS (Gemini Bio-Products) at 100,000 × *g* for 2.5 hours. Patient samples (with >90% leukemic blasts) were obtained under Oregon Health & Science University-Institutional Review Board (OHSU-IRB; Portland, OR)–approved protocol from treatment-naïve patients. Primary cells were cultured in EGM-2 media (Lonza). OP9 cells, from Dr. William H. Fleming (Oregon Health & Science University), were cultured in α-minimum essential media (Invitrogen) with 20% FBS and 60 μmol/L 2-mercaptoethanol. Igf-1r knockout (R^-) mouse embryonic fibroblasts and R^- cells expressing human insulin-like growth factor (IGF)-IR cDNA (termed R^+), provided by Drs. Briony Forbes and Douglas Yee, respectively, were cultured in Dulbecco's Modified Eagle's Medium (Invitrogen) with 10% FBS (13). Cryopreserved human $CD34^+$-enriched bone marrow cells (Stem Cell Technologies) were cultured in serum-free expansion media with the StemSpan CC110 cytokine cocktail for 5 to 7 days. All cultures contained 50 μg/mL Pen/Strep (Invitrogen). Cell lines were obtained from reliable sources without additional authentification beyond what is shown in the content of the experiments described.

Vesicle preparation and staining

Vesicles were isolated from cell lines and primary AML cells after 48 to 72 hours culture via centrifugation at 300 × *g* for 10 minutes. The supernatant was sequentially centrifuged at 2,000 × *g* for 20 minutes, at 10,000 × *g* for 20 minutes, and at 100,000 × *g* for 2 hours. The resulting pellet was washed with PBS and then centrifuged at 100,000 × *g* for 2 hours. For sucrose gradient density purification, the pellet from the first 100,000 × *g* spin was resuspended in 200 μL PBS by shaking for 4 hours at 4°C. The suspension was transferred to a sucrose step gradient (8%/15%/30%/45%/60%) and centrifuged at 150,000 × *g* for 90 minutes. The 30%/45% interface was harvested, diluted 10-fold with PBS, and the ultracentrifugation was repeated. The pellet was resuspended in 200 μL of PBS (methods adapted from ref. 8). For PKH26 (Sigma) staining, exosomes were isolated with the following changes: following the first 100,000 × *g* centrifugation, the pellet was resuspended in 1 mL PKH26 membrane dye-diluent C (Sigma) by shaking for 30 minutes at 4°C, along with a control aliquot containing diluent only.

Vesicle transfer assays

Transwell experiments were carried out in 6-well plates using 0.4-μm pore size inserts (Corning). Target cells were seeded at 2×10^4 cells per well. A total of 1 to 2×10^6 cells were added into the transwell insert and cocultured for 48 hours. Media collected from vesicle preparations after the 10,000 × *g* spin was termed vesicle-rich media (VRM). Two milliliters VRM were cocultured with 2×10^4 target cells per well in 6-well plate. Target cells were incubated with the vesicle pellets resuspended in RPMI or PBS for 48 hours in 2 mL of media, then washed twice. For real-time PCR (RT-PCR), RNA was extracted using either the RNeasy (Qiagen) or miRNeasy kit (Qiagen). Transwell cocultures with $CD34^+$ cells were not conducted because of culture media incompatibility and the limited availability of cells.

Fluorescence microscopy

Cells were exposed to 25 μL of PKH26-stained, sucrose-purified exosomes or PKH26-stained diluent C for 2 hours, followed by wash and fixation in 4% paraformaldehyde (Sigma) before treatment with Fluoromount G (Southern Biotech). Fluorescence microscopy was conducted with an Olympus IX71 microscope and DeltaVision SoftWoRx, using a ×60 1.4NA oil lens. *Z*-stacks were acquired every 0.2 μm for the complete depth of the cells. A reference bright-field image was captured from the center of each *Z*-stack. Particle quantification was conducted using ImarisCell (Bitplane, Inc.). For live-cell imaging, cells were plated on poly-L-lysine (Sigma)–coated chamber wells, treated with 5 μg/mL Hoechst 33342 and 2.5 μmol/L N-Rh-PE (Avanti Polar Lipids) for 1.5 hours followed by wash and resuspension in RPMI media with 9% horse serum (Invitrogen) and 9% FBS (Gemini Bioproducts). Images were acquired every 2.5 minutes for 2 hours, at 37°C and 5% CO_2. For colocalization studies, cells were treated with 5 μmol/L N-Rh-PE for 1 hour, fixed for 15 minutes, permeabilized with NET (NaCl + EDTA + Tris) buffer, cytospun and blocked with 2% FBS for 30 minutes at 4°C. Fixation precluded N-Rh-PE polarization seen during live cell imaging. Permeabilized cells were stained with anti-human CD63 hybridoma supernatant and anti-human Tsg101 antibodies (Abcam). AlexaFluor488 anti-mouse immunoglobulin G (IgG) and AlexaFluor647 anti-rabbit IgG (Invitrogen) were used as the secondary antibodies. Cells were stained with 4′,6-diamidino-2-phenylindole (DAPI; Invitrogen).

Transmission electron microscopy

Exosome preparations (10 μL) were deposited onto UV-activated carbon formvar 400-mesh copper grids (Ted Pella 01822-F) for 3 minutes, rinsed and stained in filtered 1.33% uranyl acetate, and then air-dried. Samples were imaged at 100 kV on a Philips CM120 transmission electron microscope. The size distribution of exosomes was determined by averaging the maximum and minimum diameters of at least 100 vesicles imaged at ×37,000 magnification.

Dynamic light scatter

Light-scattering experiments were conducted in a DynaPro molecular sizing instrument (Protein Solutions). A sample in PBS buffer was loaded into a quartz cuvette and analyzed with a 488 nm laser. Fifty spectra were collected at 25°C to estimate diffusion coefficient and relative polydispersity. Data

Published OnlineFirst November 13, 2012; DOI: 10.1158/0008-5472.CAN-12-2184

were analyzed with Dynamics software V.5.25.44 (Protein Solutions) and vesicle size was measured as the mean hydrodynamic radius.

RNA analysis and qRT-PCR

RNA was extracted using miRNeasy (Qiagen) or RNeasy (Qiagen) kits and quantified using a Nanodrop 2000c (Thermo). RNA integrity was measured using the Agilent Bioanalyzer Pico Chip or small RNA Chip (Agilent). For RT-PCR, RNAs were converted into cDNA using the SuperScript III First Strand Synthesis Kit (Invitrogen) with oligo-dT priming followed by PCR. See Supplementary Table S1 for primer sequences. For quantitative PCR (qPCR), human *IGF-IR* primers/probe (forward primer: AACTTTCTCCCTCATCGGCCG; reverse primer: GTGTGTCGCCAGCGTGTCT; probe: FAM-CGCTGATTCCTCGTGTCCGGAGG), mouse *VEGF*, mouse c-*fos*, human *GAPDH*, and mouse *GAPDH* (Applied Biosystems) were used. Relative quantification was calculated using $\Delta\Delta C_T$ algorithm with glyceraldehyde-3-phosphate dehydrogenase (GAPDH) as the endogenous control. For miRNA quantitation, TaqMan Assay Kits (Applied Biosystems) were used for reverse transcription and qRT-PCR. For PCR array analysis, reverse transcription was conducted using the RT^2 First Strand (Qiagen) Kit. PCR arrays (SABiosciences) were run according to manufacturer's instructions.

Flow-cytometry analysis

For IGF-IR detection, target R$^-$ murine embryonic fibroblasts (MEF) were trypsinized after coculture, washed, and resuspended in staining buffer (1% bovine serum albumin in PBS, w/v). Cells were stained with mouse anti-human IGF-IR-PE antibody (BioLegend) or CXCR4-APC antibody (eBioscience) × 30 minutes at 4°C, washed twice, propidium iodide (PI) was added and cells analyzed with a FACSCalibur (BD Biosciences). Data were analyzed using FlowJo software (Tree Star).

Transwell migration and cell proliferation

Ba/F3 cells were cultured for 48 hours in the presence or absence of VRM by plating 5×10^5 cells in 2 mL Ba/F3 media with 4 mL of either vesicle-rich or base media. Ba/F3 cells were washed and plated on 8-μm transwell inserts in plates containing either media alone or SDF-1α gradient. After 2 hours, transwells were removed, migrated cells were washed and counted using a Guava PCA cytometer (Millipore). For proliferation assays, 5×10^4 R$^-$ MEFs were cocultured with 1×10^6 HL-60 cells in 0.4-μm transwells for 48 hours, after which R$^-$ MEFs were counted. IGF-IR inhibitor picropodophyllin (PPP; CalBiochem) was added at 100 nmol/L before coculture.

Western blotting

Protein lysates were generated using RIPA buffer with protease inhibitors (Thermo Scientific) and protein concentrations quantified by BCA Protein Assay (Pierce). Lysates were loaded on 4% to 15% SDS-PAGE gels (Bio-Rad) for transfer and Ponceau S stain. IGF-IR was detected using rabbit anti-human IGF-IRβ (Cell Signaling Technology) and anti-rabbit IgG-HRP (Thermo Scientific). Actin was detected using mouse anti-human pan-actin (Millipore) and anti-mouse IgG-HRP (Jackson ImmunoResearch Laboratories). Chemiluminescence was detected by the Supersignal West Pico Chemiluminescent substrate (Pierce).

Results

AML cells release exosomes

To systematically examine AML vesicle release, we used several AML cell lines and patient cells. Primary AML samples phenotyped by flow-cytometry showed more than 90% of cells expressing leukemia-associated antigens (data not shown). Vesicles were isolated from culture media using differential centrifugation and sucrose gradient purification (Fig. 1A and B). Transmission electron microscopy (TEM) revealed that both HL-60 and primary AML cells released vesicles primarily between 30 and 100 nm in diameter (Fig. 1C), the size range of exosomes (9). To exclude detection method- or purification-protocol bias, we conducted dynamic light scattering (DLS) measurements comparing HL-60 vesicle preparations purified by sucrose gradient versus differential centrifugation (capturing larger vesicles; Fig. 1D). Results mirrored the TEM size and distribution profile without significant method specific bias. To show direct exosome release from AML cells, we imaged primary AML cells labeled with N-Rh-PE, a marker dye routed from the endocytic compartment to the multivesicular body (MVB) and released within exosomes (14). Representative time-lapse images from stained primary AML blasts show the polarized aggregation of dye-labeled MVB's at the plasma membrane before release of the exosome content, representative of 53% of cells in 3 primary AML samples (Fig. 1E; ref. 15). The canonical N-Rh-PE trafficking and vesicle budding provide further evidence that primary AML cells release exosomes. When we conducted immunofluorescent imaging for exosomal markers Tsg101 and CD63 (16, 17), the N-Rh-PE–stained compartment in primary AML cells colocalized with CD63 in more than 90%, with Tsg101 in 70%, and with both proteins in 29% of cells (Fig. 1F). Together, these experiments provide strong complementary evidence that AML cell lines and primary AML cells give rise to exosomes. Hereafter, we use the term "exosomes" specifically and "vesicles" generically.

Exosomes traffic mRNA between AML and stromal cells

Vesicles transfer protein and RNA between cells (18), leading us to investigate the trafficking of AML exosomes to bystander cells. To determine exosome entry, GFP-expressing murine OP9 bone marrow stromal cells were exposed to PKH26-stained exosomes from HL-60 cells (19). Fluorescence microscopy images revealed rapid and significant uptake of PKH26-stained exosomes as early as 15 minutes and increasing until 2 hours after initial exposure (Fig. 2A–F), at which time their number per cell reached a plateau (data not shown). To ascertain the transfer of specific RNA transcripts via AML exosomes, we cultured leukemia cells across a 0.4-μm transwell membrane from OP9 cells. After 48 hours of coculture, OP9 cells were harvested, RNA was

Published OnlineFirst November 13, 2012; DOI: 10.1158/0008-5472.CAN-12-2184

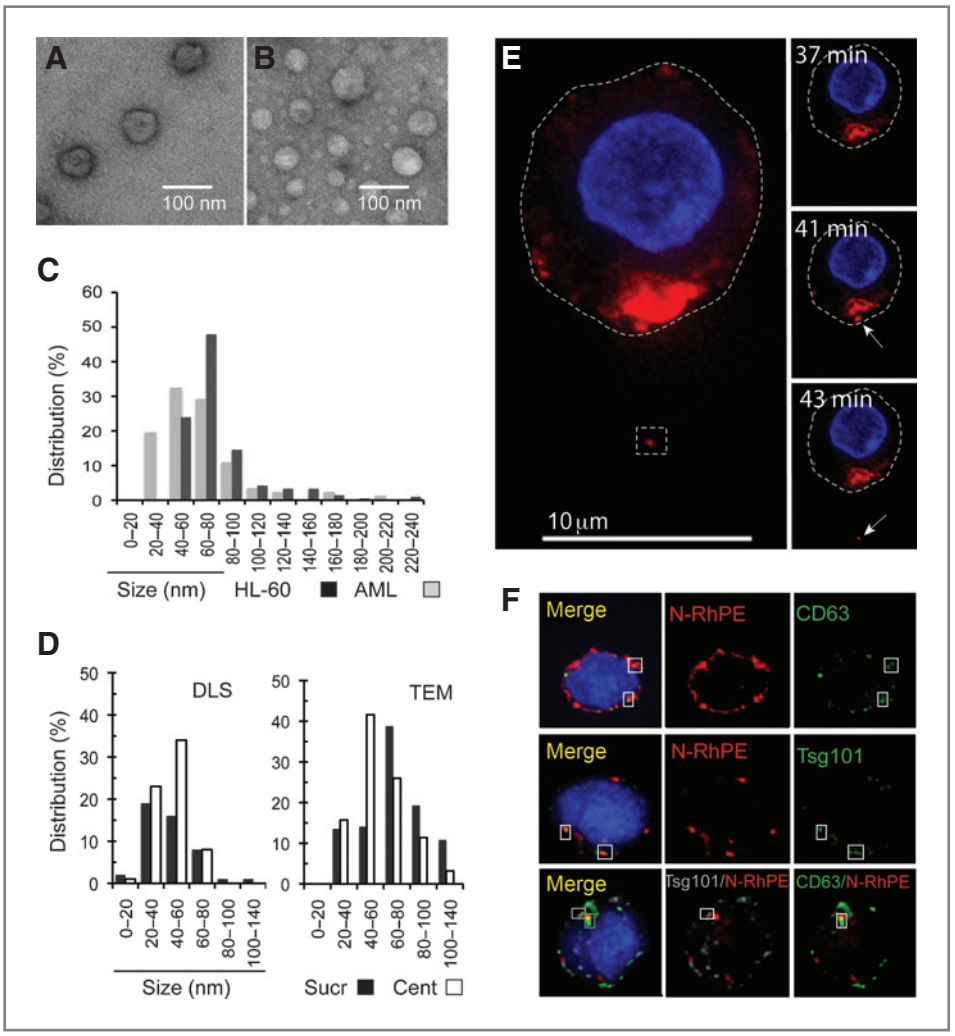

Figure 1. AML cells release exosomes. Vesicles isolated from HL-60 cells (A) and from primary AML cells (B) using sucrose gradient centrifugation, visualized by TEM. Scale bars, 100 nm. C, average diameter of more than 100 vesicles was measured from TEM of HL-60 and primary AML. D, comparison of size distribution of vesicles from sucrose gradient (Sucr) and differential centrifugation (Cent) analyzed by DLS and TEM. E, left, projection image (merged *Z*-stack) of primary cell stained with Hoechst 33342 (blue) and N-Rh-PE (red). Right, *z*-plane captured every 2.5 minutes. Dotted line, cell margin; arrows, MVB and subsequent extracellular vesicle. F, immunofluorescence of fixed primary AML cells: N-Rh-PE (red), anti-CD63 (green), anti-Tsg101 (green/white), and DAPI (blue).

extracted and reverse-transcribed. RT-PCR with species-specific primers confirmed the presence of leukemia-derived (human) CXCR-4 transcripts in murine OP9 cells after coculture with HL-60 cells or primary AML cells (Fig. 2G). These experiments show that AML exosomes transfer leukemia-derived mRNA to murine bone marrow stromal cells.

AML exosomes contain RNA with broad regulatory potential

Given the diagnostic and prognostic relevance of molecular abnormalities in AML, we decided to focus on the analysis of exosomal RNA. We initially quantified total exosome RNA among 4 leukemia cell lines, 5 different primary AML cell samples, and primary $CD34^+$ bone marrow cells. Total vesicle RNA content varied considerably among cell lines and primary AML cells after standardized culture for 48 hours (Fig. 3A). Comparing the spectrum of vesicle and cellular RNA using a bioanalyzer, we found a similar size distribution, with pronounced ribosomal and small RNA peaks (Fig. 3B). This pattern was observed in RNA obtained from cell lines and several AML samples (Fig. 3C). Because we were interested in transfer of mRNA with potential to alter the recipient cell phenotype, we used a PCR array to screen for a set of 59 transcription factors in Molm-14–derived exosomes. Many transcripts seemed either decreased or enriched relative to cellular background (adjusted for GAPDH, β-2-microbglobulin and HPRT1 controls; Fig. 3D). We selected a subset of 9 transcripts for further validation based on their involvement in hematopoiesis and/or leukemogenesis; that is, GATA1, FOXP3, SHIP1, ID1, E2F1, CEBP-α and -β, Myc, and MEF2C (20). Judged by RT-PCR, all were present in vesicle RNA from cell lines and most in primary samples, with some patient–patient variability (Fig. 3E). Our data on exosome RNA spectrum and abundance suggested strong potential for a role in AML biology.

Exosomes carry RNA transcripts with prognostic relevance in AML

Given evidence of transcript enrichment and the equilibration of vesicles between tissue compartment and bloodstream shown by others, we evaluated exosomes for AML-relevant transcripts as potential biomarkers (21–23), specifically, nucleophosmin 1 (NPM1), FLT3, CXCR4, MMP9, and

Published OnlineFirst November 13, 2012; DOI: 10.1158/0008-5472.CAN-12-2184

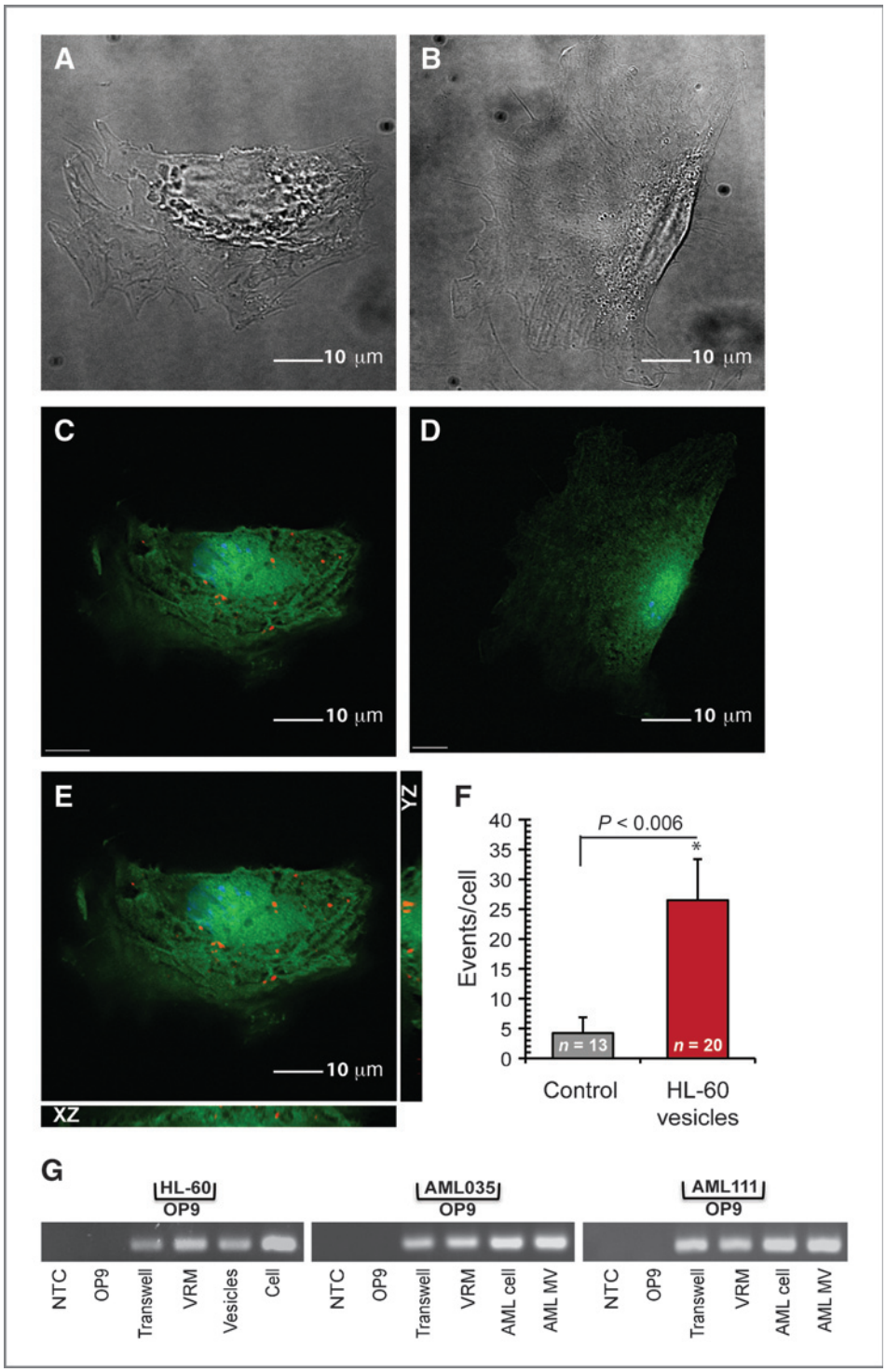

Figure 2. AML exosomes are taken up by bone marrow stromal cells. PGK-GFP OP9 cells were exposed to PKH-26–labeled HL-60 exosomes (A, C, and E) and PKH-26–labeled diluent C (B and D) for 2 hours. A and B, differential interference contrast (D DIC) images. C and D, single *z*-slices showing labeled exosomes (red). E, *Z*-stack in the *xy*-, *xz*-, and *yz*-planes. Scale bars, 10 μm. F, quantification of labeled exosomes within cells. N, number of cells analyzed; error bars, SEM; $P < 0.006$ by Student *t* test. G, RT-PCR for human CXCR4 in murine OP9s after 48 hours coculture or exposure to vesicles from HL-60 or primary AML. Transfer conditions: 0.4-μm transwell (Transwell), VRM exposure, purified vesicle exposure (vesicles). Data are representative of at least 3 independent experiments. NTC, non template control.

IGF-IR (21, 24, 25). RT-PCR analysis revealed the presence of all 5 candidate transcripts in exosomes from patient AML blasts, primary $CD34^+$ bone marrow cells, and leukemia cell lines (Fig. 4A and B and Table 1). Indeed, exosome RNA reproduced the FLT3 allelic diversity (*wt* vs. *ITD* transcripts), including multiple unique ITDs present in the bulk cell population from which they were derived (Fig. 4A and B; ref. 26). Similarly, we were able to detect transcripts bearing mutations in exon 12 of NPM1 (confirmed by sequencing and capillary gel electrophoresis) in matched exosomal and cellular RNA (Fig. 4A). We next determined relative IGF-IR transcript levels in RNA from AML patient cells and vesicles

Published OnlineFirst November 13, 2012; DOI: 10.1158/0008-5472.CAN-12-2184

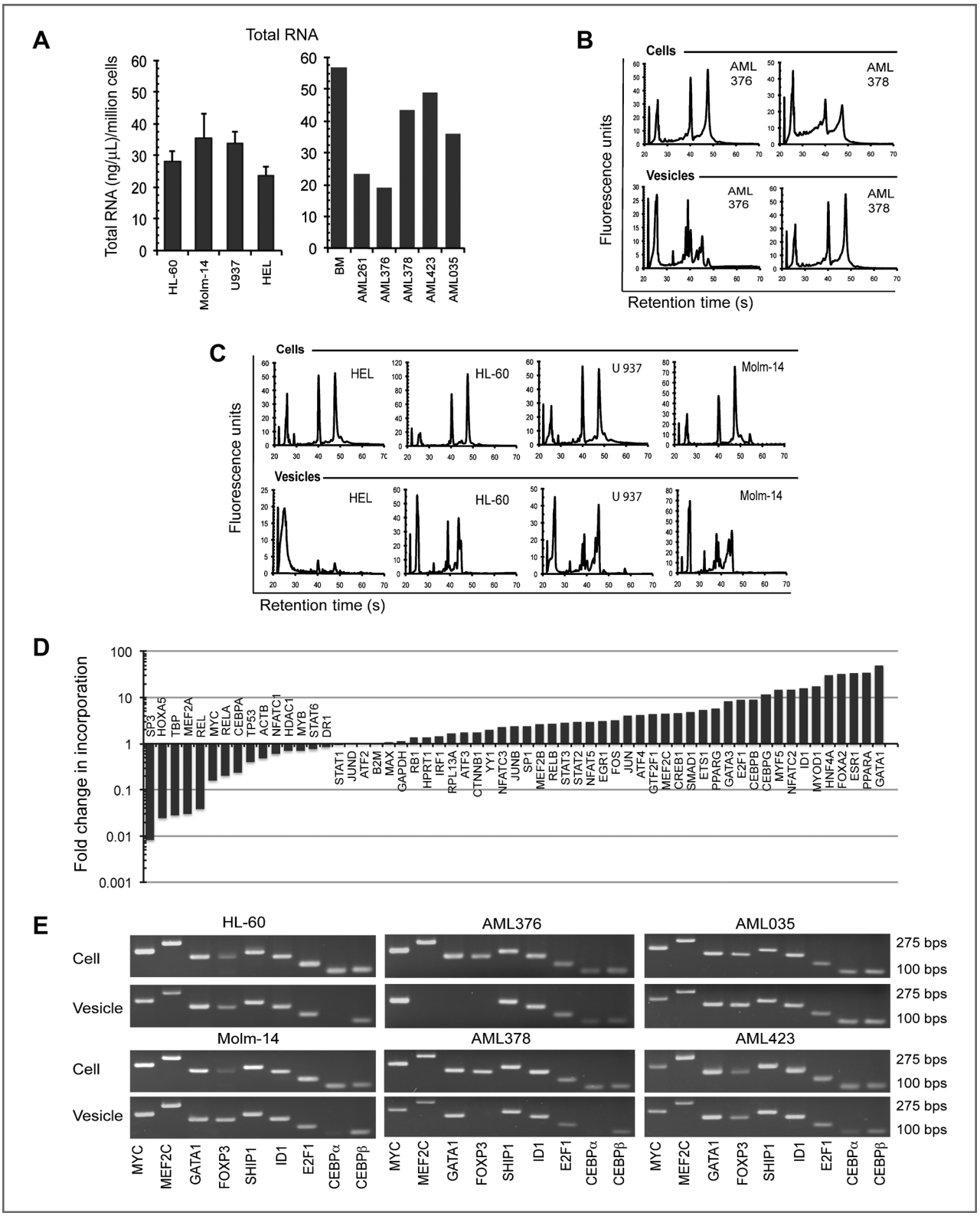

Figure 3. AML exosomes contain unique RNA profiles. A, quantification of AML or control vesicle RNA. BM: $CD34^+$ bone marrow progenitors. Data represent at least 3 individual experiments. B and C, bioanalyzer electropherograms of RNA from cells and vesicles of AML cell lines and primary samples. D, transcription factor array comparison of exosomal RNA from Molm-14 cells, expressed as fold change in vesicles versus cells. E, RT-PCR for select transcription factors in RNA from primary AML cells and vesicles from 4 patients. Data represent at least 3 individual experiments.

Published OnlineFirst November 13, 2012; DOI: 10.1158/0008-5472.CAN-12-2184

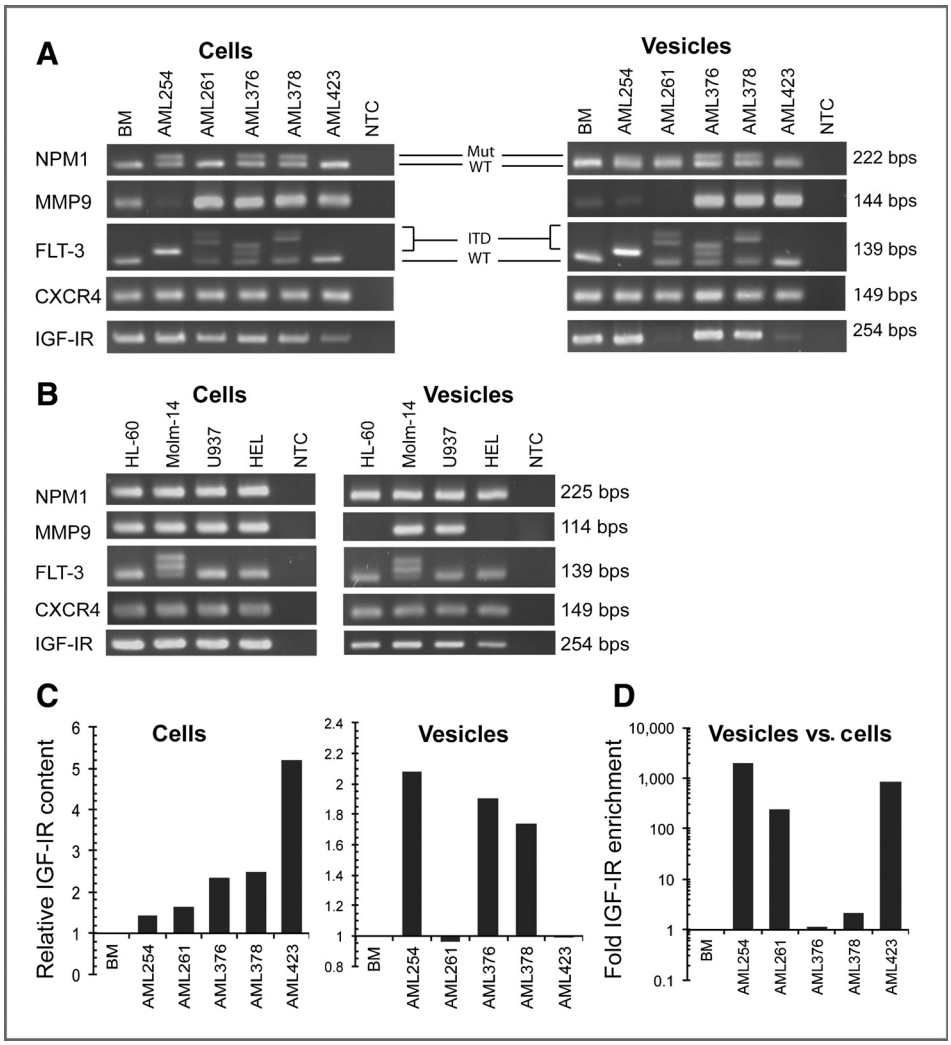

Figure 4. Leukemia-relevant transcripts in AML exosomes. RT-PCR for AML-related transcripts in cells and vesicles from primary AML samples (A) and AML cell lines (B). C, qRT-PCR for IGF-IR in primary AML cellular and vesicle RNA, normalized to $CD34^+$ bone marrow cells and vesicles. GAPDH was used as the endogenous control. D, fold enrichment of IGF-IR mRNA in vesicles versus cells, normalized to $CD34^+$ cells/vesicles.

(24, 25, 27). When normalized to GAPDH, IGF-IR mRNA levels differed substantially between primary AML samples (28). Yet, expression in both cellular and exosomal RNA was generally 2- to 5-fold higher in AML samples than in $CD34^+$ progenitors (Fig. 4C). A direct comparison of IGF-IR mRNA levels confirmed exosome enrichment over matched cellular RNA, by up to 1,000-fold in 2 of the samples tested (Fig. 4D). This relative enrichment of IGF-IR mRNA (normalized to GAPDH) seemed to be specific for leukemia-derived vesicles, as primary $CD34^+$ bone marrow vesicles exhibited IGF-IR mRNA levels proportional to those found in cells (Fig. 4D).

Transfer of IGF-IR mRNA modulates cellular responses in *Igf-Ir*-deficient cells

To show proof-of-principle for the specific functional consequences of AML exosome trafficking to bystander cells, we set up contact-independent cocultures of HL-60 or Molm-14 donor cells and (murine) OP9 target cells. Under all 3 experimental modalities (transwell coculture, vesicle-rich media exposure, and purified vesicle exposure), human-specific IGF-IR transcripts were detected in OP9 recipient cells (Fig. 5A). To determine if AML vesicle-derived IGF-IR contributes to target cell signaling after transfer, we cocultured leukemia cells across a transwell from *Igf-Ir* knockout mouse embryonic fibroblasts (R^- MEF; refs. 13, 29). In flow-cytometry analysis, R^- MEFs cocultured with HL-60, Molm-14, or U937 cells expressed human IGF-IR, although at a level less than that of R^- cells stably transfected with human *IGF-IR* cDNA (termed R^+; Fig. 5B). Protein lysates from AML cells and vesicles revealed broad differences in banding profile, reflecting the disparity between vesicle and cellular protein content that includes conventional controls, such as actin and GAPDH, or tubulin (data not shown). Even when loading 3-fold the amount of vesicle than cell protein lysate (reflected in the Ponceau S stain), significantly less actin was detected in vesicles. IGF-IR protein, as well, was present only at very low levels in AML exosomes by Western blot analysis, although it was readily detected in both WT HL-60 cells and HL-60 overexpressing IGF-IR (Fig. 5C; Supplementary Fig. S1A and S1B; ref. 30). Allowing for small amounts of IGF-IR protein in vesicles, these results nonetheless suggest that transferred human IGF-IR mRNA may be successfully translated and

Published OnlineFirst November 13, 2012; DOI: 10.1158/0008-5472.CAN-12-2184

Table 1. Transcripts detected in AML exosomes

Sample ID	Sample source	FLT-3	NPM1	IGF-IR	CXCR4	MMP9
AML10128	LA	ITD	+	+	ND	ND
AML10226	LA	ITD	+	+	ND	ND
AML10831	PB	*WT*	+	+	ND	ND
AML11009	PB	−	+	+	ND	ND
AML11105	PB	−	−	+	ND	ND
AML11254	PB	ITD	+	+	+	+
AML11261	PB	ITD	+	+	+	+
AML11376	PB	ITD	+	+	+	+
AML11378	PB	ITD	+	+	+	+
AML11423	PB	*WT*	+	+	+	+
AML12073	PB	*WT*	+	+	+	+
AML12035	BM	*WT*	+	+	+	+
NL-1	BM	WT	+	+	+	+
NL-2	BM	WT	+	+	+	+
HL-60	Cell line	*WT*	+	+	+	+
Molm-14	Cell line	ITD	+	+	+	+
U937	Cell line	*WT*	+	+	+	+
HEL	Cell line	*WT*	+	+	+	+

Abbreviations: LA, leukapheresis cells; ND, not done; NL, normal bone marrow cells; PB, peripheral blood cells; +, detected; −, not detected.

trafficked to the cell surface of R^- MEFs after coculture with AML cells. This observation is corroborated at the functional level by measuring rates of IGF-I–stimulated proliferation in R^- MEFs (13). In experiments using transwell cocultures of HL-60 with R^- MEFs, we observed increased proliferation in cocultured R^- MEFs compared with R^- MEFs alone (Fig. 5D). This proliferative response was specifically abrogated in response to the IGF-IR–specific inhibitor PPP, which similarly decreased proliferation in R^+ MEFs, indicating that the altered proliferation kinetics resulted from the transfer of IGF-IR mRNA. In addition to its mitogenic activity, IGF-IR signaling has been shown to upregulate VEGF expression (31, 32). When we assessed the effect of coculture on VEGF expression in target cells, we found that R^- MEF cells exhibited increased VEGF transcript levels by qRT-PCR following coculture with HL-60 cells (Fig. 5E). As another canonical IGF signaling response, we observed upregulation of the early response gene c-*fos* under these conditions, although this did not reach statistical significance (Fig. 5F; ref. 33). Our experiments show that exosomal transfer of IGF-IR can modulate proliferative signaling in bystander cells and promote expression of VEGF. Exosomal induction of transcripts promoting angiogenesis in bystander cells is further corroborated in the exposure of OP9 cells to Molm-14 coculture (Supplementary Fig. S2A–S2C) and Molm-14 vesicles (Supplementary Fig. S3A and S3B). We observed substantial changes in growth factor secretion into OP9 culture supernatant using commercial (murine) arrays. Despite apparent differences in secretion resulting from the presence of soluble factors under coculture conditions versus concentrated vesicle exposure, several relevant proteins whose secretion was upregulated after coculture (angiopoietin 1, endothelin 1, CXCL4, and FGF-2) were also elevated following treatment with purified vesicles. VEGF was consistently elevated after both treatments, whereas secreted osteopontin (OPN) and SDF-1 were decreased after vesicle treatment despite an increase following coculture. To validate these results (and discrepancies), we investigated several of these targets at the mRNA level with qRT-PCR, and found that while SDF-1 and VEGF mRNA tracked with secreted protein levels, OPN transcription had increased after vesicle exposure without changes in its secretion. These results illustrate hat physiologic vesicle transfer occurs in the context of other secreted effectors, which act in concert to influence surrounding cells.

miRNA enriched in AML exosomes regulates the biologic function of neighboring cells

Our initial bioanalyzer data suggested the enrichment of miRNA in exosomes (Fig. 3B and C; ref. 34). The RNA size range between 0 and 150 nts was therefore further evaluated using the small RNA bioanalyzer chip. Results confirmed abundant representation of small RNAs (defined as 0–150 nts) and miRNAs (40–80 nts; Fig. 6A). Remarkably, when comparing the calculated concentrations, we found 2-fold enrichment of small RNAs and 5- to 13-fold greater gains among miRNAs in vesicles versus parental cells across several cell lines

Published OnlineFirst November 13, 2012; DOI: 10.1158/0008-5472.CAN-12-2184

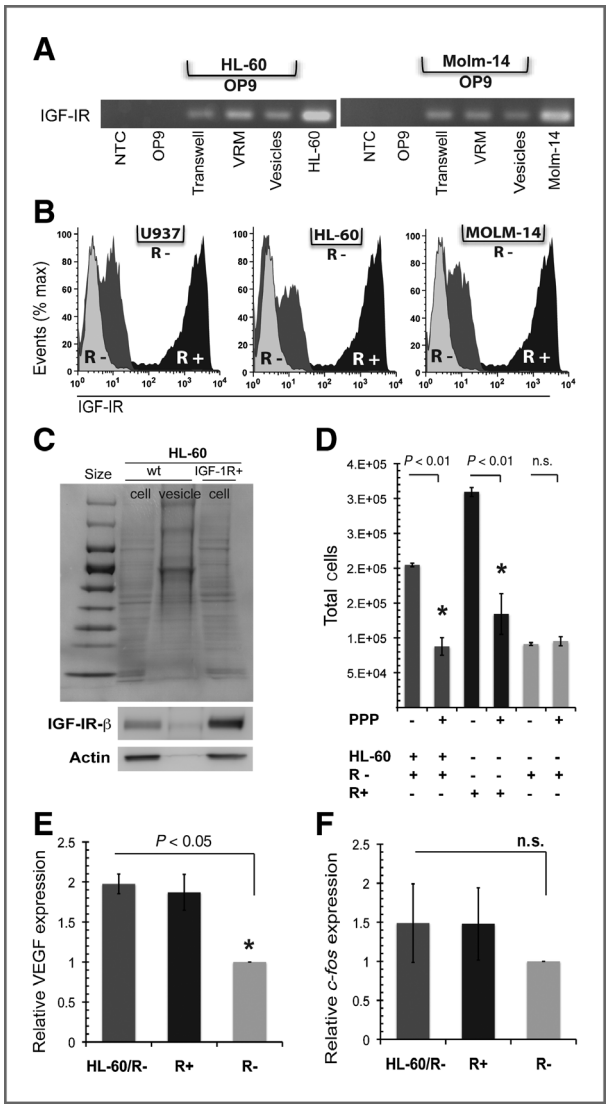

Figure 5. AML exosomes transfer leukemia-specific transcripts and modulate target cell function. A, RT-PCR for human IGF-IR mRNA in murine OP9s after 48 hours coculture or exposure to vesicles from HL-60 or MOLM-14. Transfer conditions: 0.4-μm transwell (Transwell), VRM exposure, purified vesicle exposure (vesicles). Data are representative of at least 5 independent experiments. B, flow-cytometry analysis of human IGF-IR expression in R^- MEFs after 48 hours coculture with U937, HL-60, or Molm-14. Light gray, R^- MEFs; dark gray, R^- MEFs after coculture; black, R^+ MEFs. C, top: Ponceau S stain of HL-60 cell, HL60 vesicle lysate, and cell lysate from IGF-IR overexpressing HL-60 (positive control). Bottom, Western blot analysis for IGF-IR and actin. Top and bottom, 10-μg cellular and 30-μg vesicle protein were loaded. D, proliferation of R^- MEFs after coculture with HL-60s. R^- MEFs, R^+ MEFs, or R^- MEFs/HL-60 cells were cultured with or without PPP for 48 hours. E and F, relative expression of VEGF and *c-fos* transcripts in R^- MEFs cocultured with HL-60 cells for 12 hours and in R^+ MEFs or R^- MEFs alone. Error bars, SEM. $P < 0.05$ by Student *t* test.

(Fig. 6B). We conducted qRT-PCR assays to quantify specific miRNAs in Molm-14 cells and vesicles, including Let-7a, miR-9, miR-99b, miR-150, miR-155, miR-191, and miR-223. Using the noncoding small nuclear U6 RNA for normalization, we observed significant incorporation in vesicles, ranging from 2- to near 40-fold enrichment compared with cells among this set of miRNA (Fig. 6C). When we conducted a qRT-PCR array study to profile 234 human miRNAs, our screen detected miRNAs in both Molm-14 cellular and exosomal RNA (Fig. 6D). Many miRNA were enriched in vesicles, indicated by data point skewing toward the *y*-axis, with approximately 83% of miRNAs detected in both cells and vesicles. Among miRNA represented by the array, 40 were excluded from exosomes, whereas 1 miRNA (miR-146a) was present at a detectable level only in exosomes.

One functional consequence of leukemic invasion of the niche is the displacement of hematopoietic stem and progenitor cells from the bone marrow microenvironment through altered migration and retention (4). The CXCR4/SDF-1α signaling axis plays a crucial role in this, and CXCR4 itself was recently shown to be a target of miR-150 (4, 35). We therefore examined the effect of Molm-14 exosomes (enriched in miRNA-150) on migration of Ba/F3 cells, a conditionally SDF-1α–responsive murine B-precursor cell line (36). Remarkably, Ba/F3 cells cultured for 48 hours in the presence of Molm-14–derived, vesicle-rich media and placed on 8-μm Transwell grids showed significantly decreased migration toward SDF-1α (Fig. 6E; ref. 2). Moreover, vesicle exposure specifically reduced the surface expression of CXCR4, the cognate SDF-1α receptor, by 50% as judged by median fluorescence intensity (Fig. 6F). Taken together, our results reveal that AML vesicles alter transcriptional responses, protein secretion, and migration in bystander cells.

Discussion

A specialized AML stromal niche is thought to account, in part, for the evasion of cells from therapy-induced apoptosis and is implicated in relapse (1–3). Conceptually, niche conversion requires the successive displacement and suppression of hematopoietic function and establishment of conditions conducive to leukemic spread. The mechanisms underlying this process, however, remain to be clarified (1, 4). On the basis of the established potential for exosomes to mediate cell-to-cell communication (8, 18, 37), and increasing evidence of their relevance in cancer (17, 28, 38), we investigated a role for exosomes in modulating signaling between cells in the AML microenvironment.

Classes of cell membrane–derived vesicles produced by different cell types can be distinguished on the basis of size, density, and characteristic marker proteins (39). Our studies provide compelling evidence that AML cells produce primarily exosome-sized vesicles, capable of rapid entry and cargo transfer to bystander cells. Given the importance of molecular abnormalities in AML risk stratification, we decided to examine exosomal RNA content, and observed a broad spectrum, including small RNA. Profiling the mRNA content of these vesicles revealed the presence of transcripts relevant to AML prognosis (FLT3-ITD, NPM1), treatment (FLT3-ITD, IGF-IR, CXCR4), and niche function (IGF-IR, CXCR4, MMP9; Table 1; refs. 21, 27, 40). Other experimental systems have shown that the direct cytoplasmic transfer of RNA between cells can have significant and lasting impact on cellular phenotypes

Published OnlineFirst November 13, 2012; DOI: 10.1158/0008-5472.CAN-12-2184

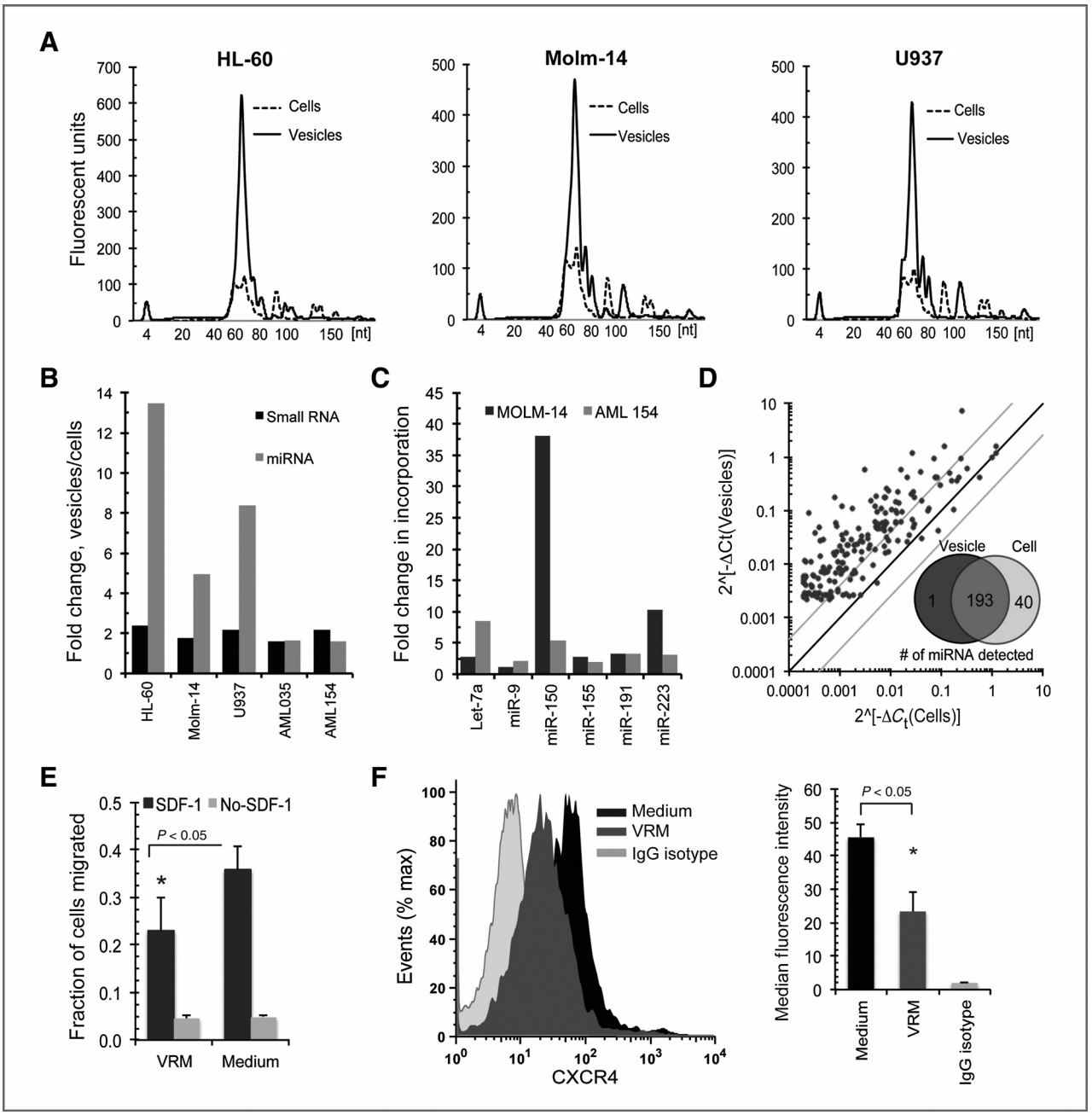

Figure 6. AML exosomes contain unique miRNA profile. A, bioanalyzer electropherograms of small RNA profiles for 3 leukemia cell lines. Major peak, small RNA. Dotted line, cellular RNA. Solid line, vesicle RNA. B, small RNA and miRNA concentrations determined by small RNA chip. C, miRNA qRT-PCR in Molm-14 vesicles versus cells, expressed as fold-change in vesicle incorporation. Data shown are representative of at least 3 independent assays. D, correlation of miRNAs in Molm-14 cells and vesicles by qPCR array, normalized to U6 snRNA. Inset, number of miRNAs unique to or shared between cells and vesicles. E, migration of Ba/F3 cells along SDF-1α gradient after 48-hour coculture with Molm-14 VRM. Data are representative of 3 independent experiments. $P < 0.05$ by Student t test. F, expression of CXCR4 on Ba/F3 cells after 48-hour exposure to Molm-14 VRM by flow cytometry. Light gray, isotype control. Dark gray, Ba/F3 after coculture. Black, control Ba/F3. Data represent 3 independent assays, $P < 0.05$ by Student t test.

(18, 19, 37, 41). Reinforcing the regulatory potential of AML exosome RNA in target cells, we found several transcription factor transcripts important to hematopoiesis and a range of AML-relevant miRNA (20).

To show the functional significance of exosome trafficking, we focused on the consequences of transfer on IGF-IR signaling in stromal cells and CXCR4 signaling in progenitor cells. Not only is IGF-IR mRNA enriched in AML exosomes, but we found that its transfer led to the induction of downstream gene expression and changes in cell proliferation that were abrogated by specific inhibition of IGF-IR kinase function. miRNA-150 was previously reported to suppress erythropoiesis and

Published OnlineFirst November 13, 2012; DOI: 10.1158/0008-5472.CAN-12-2184

target CXCR4 transcripts for degradation (35). Although both miR-150 and CXCR4 mRNA are present in AML exosomes, miR-150 is highly enriched therein, and exosome transfer to Ba/F3 progenitor cells was associated with a loss of CXCR4 surface expression and consequent decrease in cell migration toward SDF-1α. Several caveats remain: we did not titrate vesicle doses and it is possible that some of these effects will reveal exosome dose–response kinetics. At the same time, our data caution against the direct extrapolation of vesicle effects to biologic response, as both the cell coculture and VRM treatment provide further physiologic modulation via soluble factors, illustrated in Supplementary Figs. S2 and S3. This is to be expected, as the exosome transfer of a receptor, for example, would be expected to result in differential signaling events in the presence of media containing the cognate ligand. The diverse exosome cargo highlights the inherent challenge in assigning a specific functional outcome to the transfer of an individual exosomal protein or RNA transcript in the context of many others. The presence of prognostically relevant mRNA in AML-derived exosomes implies their potential development as a minimally invasive AML biomarker platform. Here, it will be important to see the extent to which specific AML exosome content will track with diagnostic parameters and change during the course of treatment.

Taken together, our results show that exosome trafficking by AML cells can alter the function of bystander cells. Our observations show the complexity of cell–cell communication and emphasize the potential impact of exosome trafficking on AML physiology. Coding and noncoding RNAs are key determinants of the cellular phenotype, and *in vitro* RNA transfer can produce experimental phenotype conversion (37, 41). The transfer of transcription factor and miRNA from AML to bystander cells presents a compelling paradigm for cell–cell communication in the leukemic niche.

Disclosure of Potential Conflicts of Interest

No potential conflicts of interest were disclosed.

Authors' Contributions

Conception and design: J. Huan, C.T. Roberts Jr, P. Kurre
Development of methodology: J. Huan, P. Kurre
Acquisition of data (provided animals, acquired and managed patients, provided facilities, etc.): J. Huan, N.I. Hornick, A.M. Skinner, N.A. Goloviznina
Analysis and interpretation of data (e.g., statistical analysis, biostatistics, computational analysis): J. Huan, N.I. Hornick, N.A. Goloviznina, C.T. Roberts Jr, P. Kurre
Writing, review, and/or revision of the manuscript: J. Huan, N.I. Hornick, A.M. Skinner, C.T. Roberts Jr, P. Kurre
Administrative, technical, or material support (i.e., reporting or organizing data, constructing databases): J. Huan, A.M. Skinner, P. Kurre
Study supervision: P. Kurre

Acknowledgments

The authors thank experimental contributions by Dr. Thomas Russell. The authors also thank Drs. Jeffrey Tyner (Oregon Health & Science University), Briony Forbes (University of Adelaide), and Douglas Yee (University of Minesota) for generous provision of cell lines.

Grant Support

This study was supported by the Friends of Doernbecher and Hyundai Hope on Wheels Foundations.

The costs of publication of this article were defrayed in part by the payment of page charges. This article must therefore be hereby marked *advertisement* in accordance with 18 U.S.C. Section 1734 solely to indicate this fact.

Received May 31, 2012; revised October 12, 2012; accepted November 5, 2012; published OnlineFirst November 13, 2012.

References

1. Ayala F, Dewar R, Kieran M, Kalluri R. Contribution of bone microenvironment to leukemogenesis and leukemia progression. Leukemia 2009;23:2233–41.
2. Zeng Z, Shi YX, Samudio IJ, Wang RY, Ling X, Frolova O, et al. Targeting the leukemia microenvironment by CXCR4 inhibition overcomes resistance to kinase inhibitors and chemotherapy in AML. Blood 2009;113:6215–24.
3. Ishikawa F, Yoshida S, Saito Y, Hijikata A, Kitamura H, Tanaka S, et al. Chemotherapy-resistant human AML stem cells home to and engraft within the bone-marrow endosteal region. Nat Biotechnol 2007;25:1315–21.
4. Colmone A, Amorim M, Pontier AL, Wang S, Jablonski E, Sipkins DA. Leukemic cells create bone marrow niches that disrupt the behavior of normal hematopoietic progenitor cells. Science 2008;322:1861–5.
5. Hatfield K, Ryningen A, Corbascio M, Bruserud O. Microvascular endothelial cells increase proliferation and inhibit apoptosis of native human acute myelogenous leukemia blasts. Int J Cancer 2006;119:2313–21.
6. Ryningen A, Wergeland L, Glenjen N, Gjertsen BT, Bruserud O. *In vitro* crosstalk between fibroblasts and native human acute myelogenous leukemia (AML) blasts via local cytokine networks results in increased proliferation and decreased apoptosis of AML cells as well as increased levels of proangiogenic Interleukin 8. Leuk Res 2005;29:185–96.
7. Kindler T, Lipka DB, Fischer T. FLT3 as a therapeutic target in AML: still challenging after all these years. Blood 2010;116:5089–102.
8. Valadi H, Ekstrom K, Bossios A, Sjostrand M, Lee JJ, Lotvall JO. Exosome-mediated transfer of mRNAs and microRNAs is a novel mechanism of genetic exchange between cells. Nat Cell Biol 2007;9:654–9.
9. Simons M, Raposo G. Exosomes–vesicular carriers for intercellular communication. Curr Opin Cell Biol 2009;21:575–81.
10. Lee TH, D'Asti E, Magnus N, Al-Nedawi K, Meehan B, Rak J. Microvesicles as mediators of intercellular communication in cancer-the emerging science of cellular 'debris'. Semin Immunopathol 2011;33:455–67.
11. Fiegl M, Samudio I, Clise-Dwyer K, Burks JK, Mnjoyan Z, Andreeff M. CXCR4 expression and biologic activity in acute myeloid leukemia are dependent on oxygen partial pressure. Blood 2009;113:1504–12.
12. Szczepanski MJ, Szajnik M, Welsh A, Whiteside TL, Boyiadzis M. Blast-derived microvesicles in sera from patients with acute myeloid leukemia suppress natural killer cell function via membrane-associated transforming growth factor-beta1. Haematologica 2011;96:1302–9.
13. Sell C, Dumenil G, Deveaud C, Miura M, Coppola D, DeAngelis T, et al. Effect of a null mutation of the insulin-like growth factor I receptor gene on growth and transformation of mouse embryo fibroblasts. Mol Cell Biol 1994;14:3604–12.
14. Willem J, ter Beest M, Scherphof G, Hoekstra D. A non-exchangeable fluorescent phospholipid analog as a membrane traffic marker of the endocytic pathway. Eur J Cell Biol 1990;53:173–84.
15. Shen B, Wu N, Yang JM, Gould SJ. Protein targeting to exosomes/microvesicles by plasma membrane anchors. J Biol Chem 2011;286:14383–95.
16. Pols MS, Klumperman J. Trafficking and function of the tetraspanin CD63. Exp Cell Res 2009;315:1584–92.

Published OnlineFirst November 13, 2012; DOI: 10.1158/0008-5472.CAN-12-2184

17. Logozzi M, De Milito A, Lugini L, Borghi M, Calabro L, Spada M, et al. High levels of exosomes expressing CD63 and caveolin-1 in plasma of melanoma patients. PLoS ONE 2009;4:e5219.
18. Al-Nedawi K, Meehan B, Micallef J, Lhotak V, May L, Guha A, et al. Intercellular transfer of the oncogenic receptor EGFRvIII by microvesicles derived from tumour cells. Nat Cell Biol 2008;10:619–24.
19. Deregibus MC, Cantaluppi V, Calogero R, Lo Iacono M, Tetta C, Biancone L, et al. Endothelial progenitor cell derived microvesicles activate an angiogenic program in endothelial cells by a horizontal transfer of mRNA. Blood 2007;110:2440–8.
20. Orkin SH, Zon LI. Hematopoiesis: an evolving paradigm for stem cell biology. Cell 2008;132:631–44.
21. Bacher U, Schnittger S, Haferlach T. Molecular genetics in acute myeloid leukemia. Curr Opin Oncol 2010;22:646–55.
22. Marcucci G, Haferlach T, Dohner H. Molecular genetics of adult acute myeloid leukemia: prognostic and therapeutic implications. J Clin Oncol 2011;29:475–86.
23. Gercel-Taylor C AS, Tullis RH, Kesimer M, Taylor DD. Nanoparticle analysis of circulating cell-derived vesicles in ovarian cancer patients. Anal Biochem 2012;428:44–53.
24. Kang HJ, Lee JW, Kho SH, Kim MJ, Seo YJ, Kim H, et al. High transcript level of FLT3 associated with high risk of relapse in pediatric acute myeloid leukemia. J Korean Med Sci 2010;25:841–5.
25. Doepfner KT, Boller D, Arcaro A. Targeting receptor tyrosine kinase signaling in acute myeloid leukemia. Crit Rev Oncol Hematol 2007; 63:215–30.
26. Cheung AM, Chow HC, Kwong YL, Liang R, Leung AY. FLT3/internal tandem duplication subclones in acute myeloid leukemia differ in their engraftment potential in NOD/SCID mice. Leuk Res 2010;34:119–22.
27. Chapuis N, Tamburini J, Cornillet-Lefebvre P, Gillot L, Bardet V, Willems L, et al. Autocrine IGF-1/IGF-1R signaling is responsible for constitutive PI3K/Akt activation in acute myeloid leukemia: therapeutic value of neutralizing anti-IGF-1R antibody. Haematologica 2010;95: 415–23.
28. Keller S, Ridinger J, Rupp AK, Janssen JW, Altevogt P. Body fluid derived exosomes as a novel template for clinical diagnostics. J Transl Med 2011;9:86.
29. Coppola D, Ferber A, Miura M, Sell C, D'Ambrosio C, Rubin R, et al. A functional insulin-like growth factor I receptor is required for the mitogenic and transforming activities of the epidermal growth factor receptor. Mol Cell Biol 1994;14:4588–95.
30. Atay S, Gercel-Taylor C, Kesimer M, Taylor DD. Morphologic and proteomic characterization of exosomes released by cultured extravillous trophoblast cells. Exp Cell Res 2011;317:1192–202.
31. Mitsiades CS, Mitsiades NS, McMullan CJ, Poulaki V, Shringarpure R, Akiyama M, et al. Inhibition of the insulin-like growth factor receptor-1 tyrosine kinase activity as a therapeutic strategy for multiple myeloma, other hematologic malignancies, and solid tumors. Cancer Cell 2004;5:221–30.
32. Rajski M, Zanetti-Dallenbach R, Vogel B, Herrmann R, Rochlitz C, Buess M. IGF-I induced genes in stromal fibroblasts predict the clinical outcome of breast and lung cancer patients. BMC Med 2010;8:1.
33. Muller R, Bravo R, Burckhardt J, Curran T. Induction of c-fos gene and protein by growth factors precedes activation of c-myc. Nature 1984;312:716–20.
34. Chen TS, Lai RC, Lee MM, Choo AB, Lee CN, Lim SK. Mesenchymal stem cell secretes microparticles enriched in pre-microRNAs. Nucleic Acids Res 2010;38:215–24.
35. Tano N, Kim HW, Ashraf M. microRNA-150 regulates mobilization and migration of bone marrow-derived mononuclear cells by targeting Cxcr4. PLoS ONE 2011;6:e23114.
36. Jacobi A, Thieme S, Lehmann R, Ugarte F, Malech HL, Koch S, et al. Impact of CXCR4 inhibition on FLT3-ITD-positive human AML blasts. Exp Hematol 2010;38:180–90.
37. Ratajczak J, Miekus K, Kucia M, Zhang J, Reca R, Dvorak P, et al. Embryonic stem cell-derived microvesicles reprogram hematopoietic progenitors: evidence for horizontal transfer of mRNA and protein delivery. Leukemia 2006;20:847–56.
38. Ghosh AK, Secreto CR, Knox TR, Ding W, Mukhopadhyay D, Kay NE. Circulating microvesicles in B-cell chronic lymphocytic leukemia can stimulate marrow stromal cells: implications for disease progression. Blood 2010;115:1755–64.
39. Thery C, Zitvogel L, Amigorena S. Exosomes: composition, biogenesis and function. Nat Rev Immunol 2002;2:569–79.
40. Olsnes AM, Hatfield KJ, Bruserud O. The chemokine system and its contribution to leukemogenesis and treatment responsiveness in patients with acute myeloid leukemia. J BUON 2009;14(Suppl 1): S131–40.
41. Del Tatto M, Ng T, Aliotta JM, Colvin GA, Dooner MS, Berz D, et al. Marrow cell genetic phenotype change induced by human lung cancer cells. Exp Hematol 2011;39:1072–80.

Cancer Research
The Journal of Cancer Research (1916–1930) | The American Journal of Cancer (1931–1940)

AACR American Association for Cancer Research

RNA Trafficking by Acute Myelogenous Leukemia Exosomes

Jianya Huan, Noah I. Hornick, Matthew J. Shurtleff, et al.

Cancer Res Published OnlineFirst November 13, 2012.